Alternate deacylating specificities of the archaeal sirtuins Sir2Af1 and Sir2Af2

Alison E. Ringel,[1] Christina Roman,[2] and Cynthia Wolberger[1,2]*

[1]Department of Biophysics and Biophysical Chemistry, Johns Hopkins University School of Medicine, Baltimore, Maryland 21205-2185
[2]The Howard Hughes Medical Institute, Johns Hopkins University School of Medicine, Baltimore, Maryland 21205-2185

ABSTRACT: Sirtuins were originally shown to regulate a wide array of biological processes such as transcription, genomic stability, and metabolism by catalyzing the NAD^+-dependent deacetylation of lysine residues. Recent proteomic studies have revealed a much wider array of lysine acyl modifications *in vivo* than was previously known, which has prompted a reevaluation of sirtuin substrate specificity. Several sirtuins have now been shown to preferentially remove propionyl, succinyl, and long-chain fatty acyl groups from lysines, which has changed our understanding of sirtuin biology. In light of these developments, we revisited the acyl specificity of several well-studied archaeal and bacterial sirtuins. We find that the *Archaeoglobus fulgidus* sirtuins, Sir2Af1 and Sir2Af2, preferentially remove succinyl and myristoyl groups, respectively. Crystal structures of Sir2Af1 bound to a succinylated peptide and Sir2Af2 bound to a myristoylated peptide show how the active site of each enzyme accommodates a noncanonical acyl chain. As compared to its structure in complex with an acetylated peptide, Sir2Af2 undergoes a conformational change that expands the active site to accommodate the myristoyl group. These findings point to both structural and biochemical plasticity in sirtuin active sites and provide further evidence that sirtuins from all three domains of life catalyze noncanonical deacylation.

Keywords: sirtuins; deacetylation; deacylation; crystallography

*Correspondence to: Cynthia Wolberger, Department of Biophysics and Biophysical Chemistry, Johns Hopkins University School of Medicine, 725 N. Wolfe St., Baltimore, MD 21205. E-mail:cwolberg@jhmi.edu

Introduction

Lysine acetylation is an abundant and well-studied post-translational modification that regulates a broad array of cellular processes in organisms ranging from bacteria to mammals.[1–3] In addition to identifying specific acetylation sites,[4,5] advances in mass spectrometry have also revealed a surprisingly broad array of lysine acyl modifications *in vivo* whose chemical properties differ from acetylation. Studies in eukaryotes have identified modifications such as propionylation,[6] butyrylation,[6] crotonylation,[7] malonylation,[8,9] succinylation,[10] and glutarylation[11] decorating lysine residues. Although it remains to be seen how many of these acyl modifications are conserved throughout evolution, widespread lysine succinylation has been detected in *E. coli*[12,13] and lysine propionylation has been discovered in *Salmonella enterica*.[14] Acyl chain identity is increasingly recognized as an additional factor in regulating cellular activities, and there are

R:

Acetyl-

Propionyl-

Butyryl-

Succinyl-

Myristoyl-

NAD^+ = **N**icotinamide **A**denine **D**inucleotide
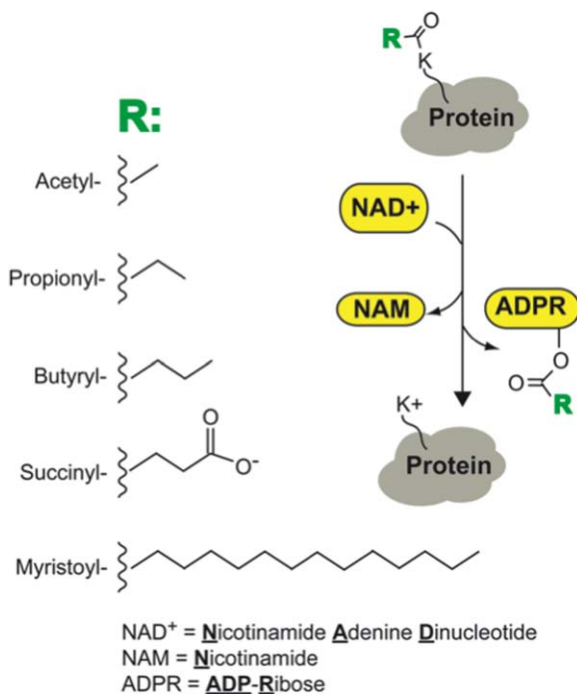NAM = **N**icotinamide
ADPR = **ADP**-**R**ibose

Figure 1. Summary of the sirtuin deacylation reaction and chemical structures of various lysine acyl modifications found in cells.

now examples of lysine residues that can be modified by more than one type of acyl chain *in* vivo.[12,15,16] Identifying the enzymes that attach and remove different types of lysine acyl modifications is therefore a key aspect in elucidating regulatory pathways.

Sirtuins were initially identified as a class of NAD^+-dependent deacetylases conserved across all three domains of life,[17–19] where they regulate a remarkably broad range of cellular processes. Sirtuins catalyze lysine deacetylation by cleaving nicotinamide from NAD^+ and generating a mixture of 2′ and 3′-O-acetyl-ADP ribose in addition to the unmodified lysine (Fig. 1). The founding member of the sirtuin family, yeast Sir2, regulates transcriptional silencing by deacetylating histones and promoting the formation of heterochromatin.[20] CobB, a bacterial homolog of yeast Sir2, regulates signal transduction pathways,[21] the activity of metabolic enzymes,[14,22,23] and mRNA transcription.[24–26] The seven human sirtuins also regulate a wide variety of processes including the response to oxidative stress, fatty acid oxidation, genome stability, and transcription.[27,28] Because of the central roles that sirtuins play in so many critical pathways across biology, these enzymes have been the subjects of intense study.[27,29,30]

Although biological functions of sirtuins were originally ascribed to their deacetylation activity, recent studies have shown that several sirtuins are more active *in vitro* in removing other types of lysine acyl modifications,[11,16,31,32] and that these alternate specificities are important for their biological roles.[11,16,31] In some cases, sirtuins that have little or no deacetylase activity *in vitro* were shown to be more active against longer or charged acyl chains, pointing to acyl group identity as an important component of sirtuin specificity.[9,16,31–33] For example, human SIRT5 preferentially removes negatively charged succinyl, malonyl, and glutaryl acyl groups from lysines.[9,11,16] This activity is important for SIRT5 regulation of the enzyme, carbamoyl phosphate synthase (CPS1), which is desuccinylated[16] and deglutarylated[11] by SIRT5 *in vivo*. Desuccinylation by SIRT5 also regulates the activity of the pyruvate dehydrogenase and succinate dehydrogenase complexes in mouse embryonic fibroblasts,[34] as well as the activity of Cn/Zn superoxide dismutase (SOD1) in human cells.[35] A crystal structure of human SIRT5 bound to a succinylated peptide has revealed the molecular basis for preferential removal of these negatively charged acyl modifications.[16]

Human SIRT6 also exhibits alternate acyl chain specificity, preferentially removing long chain fatty acyl groups from lysine.[31,33] SIRT6 deacetylates histone H3K9[36] and PGC1-α *in vivo*[37]; however, the rate at which SIRT6 deacetylates lysines *in vitro* is markedly lower than the rate for removal of long-chain fatty acyl modifications, including myristoyl groups.[31,33] A biological target for SIRT6 demyristoylating activity has been identified in mammalian cells, where SIRT6-demyristoylates the cytokine, TNF-α, promoting its secretion.[31] PfSir2a, a sirtuin from the malaria parasite *P. falciparum*, also has robust demyristoylating and low deacetylating activities,[32] although the underlying biology for PfSir2a remains to be elucidated. The bacterial sirtuin, CobB, has multiple deacylating activities that are biologically relevant. In addition to its deacetylation activity, which regulates the activity of acetyl CoA synthetase,[22] CobB also regulates propionyl-CoA synthetase (PrpE) activity by depropionylating the enzyme *in vivo*[14] and was recently shown to have desuccinylating activity.[13] These findings emphasize the importance of alternative sirtuin deacylation activities in diverse biological pathways.

Structural studies of sirtuins bound to different substrates have provided clues to their true acyl specificities as well as insights into how their active sites accommodate noncanonical acyl modifications. The structure of human SIRT5 in complex with a thioacetylated peptide revealed a negatively charged CHES buffer molecule in the active site,[16] which provided a clue that SIRT5 might also remove negatively charged acyl modifications.[16] Biochemical assays confirmed this hypothesis, while a structure of SIRT5 in complex with a succinylated peptide revealed that the succinyl carboxylate was contacted by the same residues that bound the negatively charged buffer molecule.[16] Structures of the demyristoylating enzymes, human SIRT6 and *P. falciparum*

PfSir2A, bound to myristoylated peptides show how long hydrophobic tunnels near these sirtuins' active sites accommodate the long aliphatic chain of the myristoyl group and explain why these enzymes preferentially remove long acyl chains.[31,32] These studies highlight the important clues that structures can shed on the true acyl specificities of sirtuins.

In light of the recent findings that some sirtuins have alternative deacylation activities that are important for their function, we revisited the substrate preferences of several bacterial and archaeal enzymes that have been used as model systems to study the structure-based mechanism of the sirtuin deacetylation reaction.[38–42] Sir2Af1 and Sir2Af2 from *Archaeoglobus fulgidus*, TmSir2 from *Thermotoga maritima* and CobB from *Escherichia coli* were tested against a panel of peptides containing different acyl modifications. Of the enzymes tested, only TmSir2 preferred acetylated substrates, whereas the other three enzymes exhibited alternate acyl chain specificities. Crystal structures of Sir2Af1 bound to a succinylated peptide and Sir2Af2 bound to a myristoylated peptide reveal features of the substrate-binding pocket that govern the specificity of each sirtuin for its preferred acyl modification. Interestingly, Sir2Af2 undergoes a conformational change that enables it to accommodate the long myristoyl group. These studies underscore the principle that sirtuins are a family of deacylases rather than deacetylases and reveal principles for structure based modeling of sirtuin acyl group specificity.

Results

Structure-based prediction of acyl chain specificity for Sir2Af1 and Sir2Af2

In light of the chemically diverse array of lysine acyl modifications that have been detected in cells and the recently discovered ability of some sirtuins to remove these modifications, we speculated that the archaeal sirtuins, Sir2Af1 and Sir2Af2, might preferentially remove acyl modifications from lysine other than acetyl groups. Structures of these sirtuins bound to a variety of substrates have been previously reported. These include structures of Sir2Af1 bound to NAD^+,[39,43] and of Sir2Af2 bound to an acetylated peptide[38] as well as in complex with NAD^+-derived metabolites.[41,44] Although both enzymes deacetylate peptides and proteins *in vitro*,[38,39,43] comparisons with structures of SIRT5[16] and SIRT6[31] suggested that Sir2Af1 and Sir2Af2 might also remove other types of acyl modifications.

Sir2Af1 contains features in common with SIRT5 that are consistent with a preference for removing negatively charged acyl groups from lysine. Recent structural studies of the human demalonylating and desuccinylating enzyme, SIRT5, identified tyrosine and arginine residues (Y102 and R105) that confer specificity for the negatively charged succinyl group.[16] Y102 donates a hydrogen bond to the modified lysine, while the R105 guanidinium group participates in both electrostatic and hydrogen bonding interactions with the succinyl carboxylate.[16] Interestingly, SIRT5 is the only human sirtuin where these residues are conserved,[16] and biochemical studies have confirmed that the other human sirtuins are weak desuccinylases *in vitro*.[33] Kinetically, SIRT5 is remarkably specific for removing negatively charged acyl modifications, as its K_m decreases by two orders of magnitude when supplied with succinyl or malonyl lysine compared to acetyl lysine,[16] which translates into an increase of nearly three orders of magnitude in the specificity constant, k_{cat}/K_m.[16] Not only are these two residues conserved in Sir2Af1 as well as in the desuccinylating enzyme, *E. coli* CobB [Fig. 2(a)],[13] but they are also strongly evolutionarily coupled.[45] A single point mutation of a corresponding residue in Sir2Af2 (M70R) profoundly alters its specificity, conferring desuccinylating activity on the mutant Sir2Af2-M70R while decreasing deacetylation activity.[45] We therefore hypothesized that Sir2Af1 is a desuccinylating enzyme.

A previously reported crystal structure of Sir2Af2[38] contains a serendipitously bound PEG molecule [Fig. 2(b)] that suggests that Sir2Af2 may be able to remove medium to long fatty acyl modifications. Three of the five monomers within the crystal asymmetric unit contain a long PEG molecule that binds in a hydrophobic tunnel that extends away from the acetyl lysine binding site.[44] The PEG molecules align remarkably well with the myristoyl group in structures of both SIRT6 and PfSir2a bound to myristoylated peptides [Fig. 2(b)],[31,32] suggesting that Sir2Af2 may also accommodate long fatty acyl chains and thus catalyze lysine demyristoylation.

Alternative deacylating activities of archaeal and bacterial sirtuins

To test our hypothesis that Sir2Af1 removes negatively charged acyl modifications while Sir2Af2 has demyristoylating activity, we assayed the activity of these enzymes on peptides based on the sequence of histone H4 containing acetyl, propionyl, butyryl, succinyl, or myristoyl lysine at residue K16 (Fig. 1). As a comparison, we also tested the bacterial sirtuin, TmSir2, from *Thermotoga maritima*, whose active site cannot accommodate larger acyl groups and is thus predicted to be a *bona fide* deacetylase,[46,47] and *E. coli* CobB, which desuccinylates peptides *in vitro*.[13]

Using an assay that monitors NAD^+ consumption,[38] we found that Sir2Af1 activity is approximately fivefold higher against succinyl lysine as compared to acetyl lysine [Fig. 3(a), Supporting Information Table I). As previously observed, the overall activity of Sir2Af1 is weak as compared to
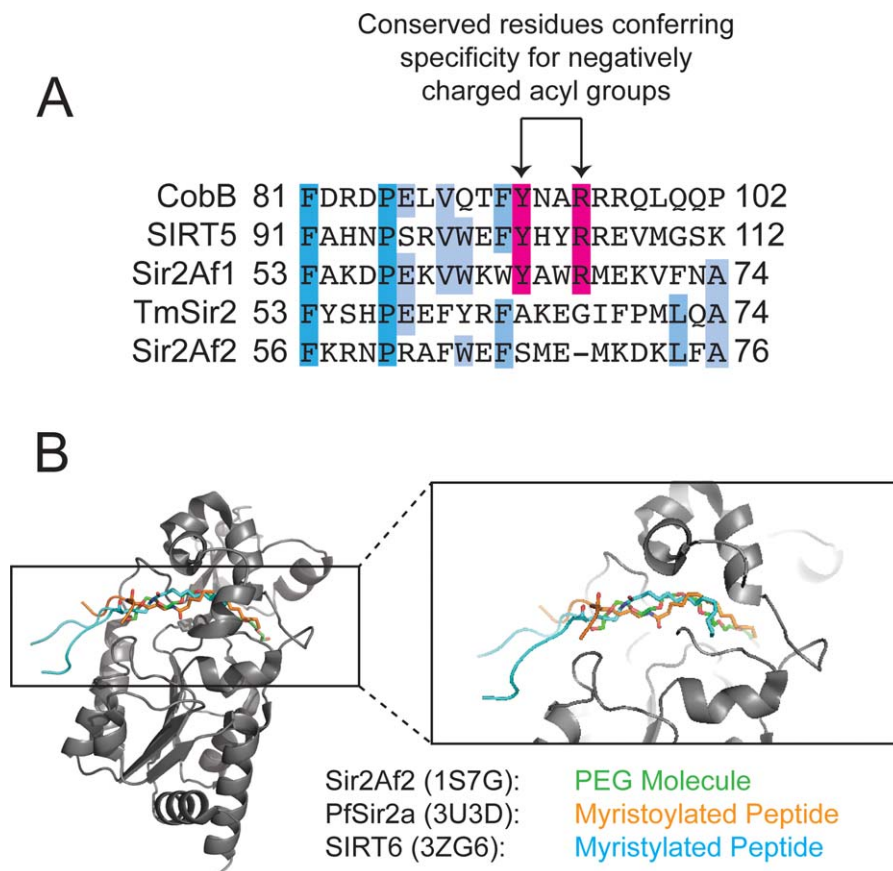
Figure 2. Structure- and sequence-guided predictions of acyl chain specificity. (a) Sequence alignment between sirtuins that are specific for negatively charged acyl chains (CobB, SIRT5, and Sir2Af1) and those that are not (Sir2Af2 and TmSir2). Conserved tyrosine and arginine residues confer specificity for negatively charged acyl modifications to lysine.[13,16] (b) Structural alignment between human SIRT6 and PfSir2a, which are both demyristoylating enzymes, and Sir2Af2. All three ligands are shown, but only the Sir2Af2 structure is displayed. Both myristoyl lysine residues overlay with a PEG molecule from the Sir2Af2 structure, suggesting alternate specificity for Sir2Af2.

other archaeal and bacterial sirtuins.[39] We confirmed that NAD^+-consumption by Sir2Af1 reflects peptide desuccinylation using an HPLC-based assay that monitors the peptide directly [Fig. 3(b)], demonstrated by a shift in its retention time in the presence of enzyme and NAD^+. CobB also exhibits robust desuccinylating activity in our assay, as it desuccinylates peptides at a rate ∼2.3-fold faster than deacetylation [Fig. 3(a), Supporting Information Table I). Interestingly, CobB activity was lower on the uncharged acyl modifications, propionyl and butyryl, which are smaller than succinyl groups and would be expected to be accommodated in the same binding pocket. CobB depropionylates substrates 1.8-fold more slowly and debutyrylates 3-fold more slowly than deacetylation of the same peptide; no demyristoylating activity was detected [Fig. 3(a), Supporting Information Table I).

We next tested the prediction that the archaeal sirtuin Sir2Af2 would preferentially remove long fatty acyl modifications. Consistent with our hypothesis, Sir2Af2 shows increased reaction velocity with increasing acyl chain length [Fig. 3(a), Supporting Information Table I). As compared to its deacetylating activity, Sir2Af2 depropionylated, debutyrylated, and demyristoylated a peptide of the same sequence at 1.5-, 1.9-, and 3.4-fold higher rates, respectively [Fig. 3(a), Supporting Information Table I). Even though the carbon backbone for succinyl lysine is substantially shorter in length than myristoyl lysine, Sir2Af2 had no detectable desuccinylating activity, suggesting that its active site can accommodate substrates that are long and hydrophobic but not charged. To confirm that NAD^+-consumption reflects peptide deacylation, we monitored reaction progress using an HPLC-based assay [Fig. 3(b)].

We also examined the acyl specificity of the bacterial sirtuin, TmSir2, which we expected to preferentially remove acetyl groups as compared to other acyl modifications based on previous structural and biochemical data. Structures of TmSir2 bound to both acetylated[46] and propionylated peptides[47] have been reported, showing that the modified lysine fits snugly into a tight hydrophobic pocket. In addition,
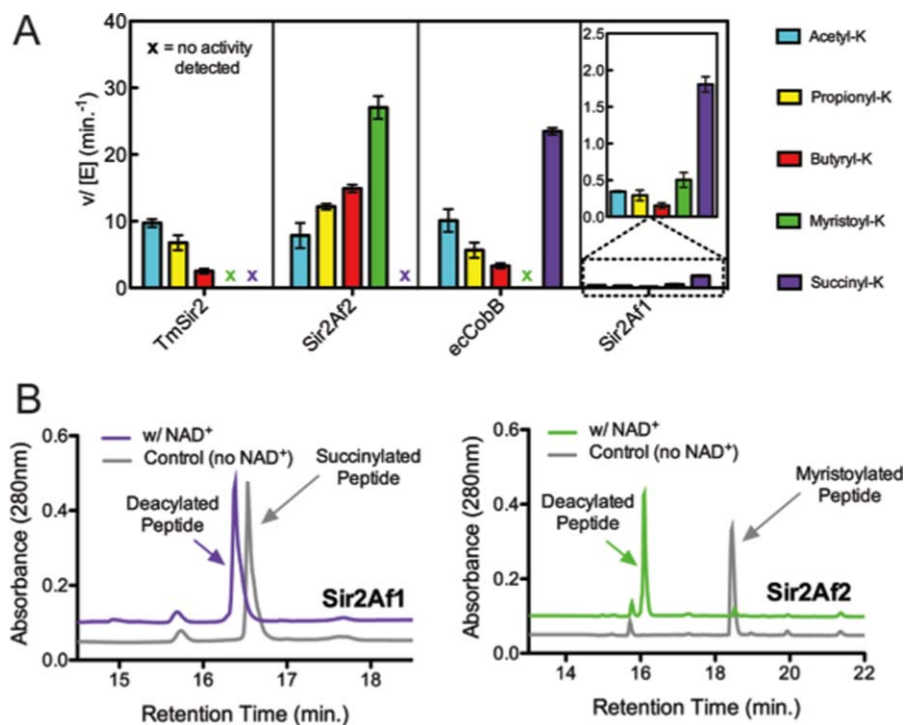
Figure 3. Comparison of deacylation activities of bacterial and archaeal sirtuins. (a) Rates of NAD$^+$-consumption were measured for different sirtuin enzymes against 250 μM acylated histone H4 peptide.[5] TmSir2, Sir2Af2, and CobB were used at a concentration of 2 μM, and Sir2Af1 was used at a concentration of 15 μM. Initial rates were normalized to total enzyme concentration for comparison. (b) HPLC chromatograms from deacylation reactions. Left: 15 μM Sir2Af1 was incubated with 250 μM succinylated H4 peptide for 1 h at 50°C. Right: 2 μM Sir2Af2 was incubated with 250 μM myristoylated H4 peptide for 20 min at 50°C. The peptides were deacylated only when 2 mM NAD+ was added, causing them to elute at an earlier retention time.

TmSir2 was previously shown to catalyze depropionylation more slowly than deacetylation.[47] Consistent with previous data, TmSir2 preferentially removed acetyl groups, with relatively lower activity on all other acyl modifications tested [Fig. 3(a), Supporting Information Table I]. No activity was detectable against myristoyl lysine or succinyl lysine [Fig. 3(a), Supporting Information Table I].

Crystal structure of Sir2Af1 bound to a succinylated peptide

To determine the structural basis of Sir2Af1 specificity for negatively charged acyl chains, we solved the structure of Sir2Af1 sirtuin bound to a succinylated H4 peptide at 1.8 Å resolution (PDB ID 4TWI). Crystallographic statistics are summarized in Table I. The overall structure resembles a previously reported structure of Sir2Af1 bound to NAD$^+$ [Fig. 4(a)].[39] Electron density 2Fo-Fc maps [Fig. 4(b)] and simulated annealing omit maps show unambiguous density for the succinylated lysine [Fig. 4(c)]. Conserved arginine and tyrosine residues, Y64 and R67 [Fig. 2(a)], hydrogen bond and form electrostatic interactions with the succinyl carboxylate [Fig. 4(d)] in the same way that SIRT5 engages a succinylated peptide [Fig. 4(e)].[16] Although CobB has not been crystallized bound to a succinylated substrate, it

likely uses the same interactions to bind negatively charged acyl chains. If a succinyl group is modeled into its structure in complex with an acetylated peptide,[40] a single rotamer change by residue R95 can recapitulate the hydrogen bonding network found in the active sites of Sir2Af1 and SIRT5 [Fig. 4(f)].

Crystal structure of Sir2Af2 bound to a myristoylated peptide

To elucidate how Sir2Af2 accommodates long acyl chains in its active site, we determined the structure of Sir2Af2 bound to a myristoylated peptide at a resolution of 1.65 Å (PDB ID 4TWJ) [Fig. 5(a)]. Crystallographic statistics are summarized in Table I. The structure resembles previously reported structures of Sir2Af2 bound to an acetylated p53 peptide,[38] NAD$^+$, or ADP ribose.[44] Electron density for the myristoylated peptide is clearly observable in both 2Fo-Fc and in simulated annealing omits maps [Fig. 5(b)]. As predicted, the myristoyl group occupies a hydrophobic tunnel in the Sir2Af2 active site where a PEG molecule was located in a previous structure.[44] An alignment with crystal structures of other sirtuins in complex with myristoylated peptides (human SIRT6[31] and PfSir2a[32]) shows that the myristoyl groups from all three structures overlay

Table I. *Crystallographic data collection and refinement statistics.*

	Diffraction data	
	Sir2-Af1 bound to a succinylated peptide	Sir2-Af2 bound to a myristoylated peptide
Space group	P2$_1$	P2$_1$
Wavelength (Å)	1.54	1.033
Unit cell dimensions		
a, b, c (Å)	44.61, 51.36, 57.69	38.48, 77.25, 45.90
α, β, γ (°)	90.0, 101.9, 90.0	90.0, 110.7, 90.0
Resolution (Å)	21.94-1.79 (1.85-1.79)	42.93 - 1.65 (1.71 - 1.65)
Measured reflections	53220 (2921)	99631 (8711)
Unique reflections	23269 (2008)	30123 (2941)
Completeness (%)	95.39 (83.73)	99.73 (97.89)
Average *I*/σ (merged reflections)	7.36 (1.85)	13.24 (4.15)
Multiplicity	2.3 (1.5)	3.3 (3.0)
R_{merge} (%)	11.7 (33.9)	5.01 (18.3)
	Refinement Statistics	
Total atoms	2213	2139
Protein	1968	1906
Ligands	7	33
Water	238	200
CC1/2	0.977 (0.751)	0.997 (0.949)
CC*	0.994 (0.926)	0.999 (0.987)
R_{work} (%)/R_{free} (%)	19.2/ 22.1	18.0/ 20.6
	B-factors	
Protein	18.1	18.2
Ligands	39.6	32.9
Solvent	29.9	33.0
	RMSD	
Bond lengths (Å)	0.005	0.005
Bond angles (°)	1.00	1.02

Values in parentheses correspond to data from the highest resolution shell.

well, suggesting a conserved function for the hydrophobic tunnel [Fig. 5(c)].

In contrast with Sir2Af1, which does not require a conformational change to bind succinyl lysine, the substrate-binding pocket of Sir2Af2 must rearrange in order to accommodate a myristoyl group. If a myristoyl lysine is docked into the structure of Sir2Af2 bound to an acetylated peptide,[38] a kinked helix obstructs the path of the acyl chain through the hydrophobic tunnel [Fig. 5(d)]. Two residues, L74 and F75, are located on the kinked helix and sterically occlude the part of the hydrophobic tunnel that is furthest from the active site in the structure of Sir2Af2 bound to an acetylated peptide [Fig. 5(e)].[38] Superposition with the structure reported here shows that the terminal six carbons of the myristoyl chain would clash with these two residues [Fig. 5(e)]. However, in the structure of Sir2Af2 bound to a myristoylated peptide, the helix straightens out, thereby moving the α-carbons of L74 and F75 by 5.2 Å and 8.3 Å, respectively [Fig. 5(e)]. This widens the tunnel by more than 6 Å, allowing Sir2Af2 to accommodate the full length of the myristoyl chain [Fig. 5(e)].

Discussion

Renewed interest in sirtuin substrate preference has been triggered by recent studies that have revealed

the presence of a large and chemically diverse repertoire of acyl modifications in cells. For a growing number of sirtuins, the ability to remove acyl modifications other than acetyl groups has been implicated in their biological roles. Determining the true specificities of sirtuins for different acyl chains is thus essential to understanding the roles of sirtuins in biology. Here we have revisited the acyl chain specificity of two archaeal enzymes that were previously used as models for understanding the sirtuin deacetylation reaction and showed that both enzymes preferentially remove other types of acyl modifications. Sir2Af1 preferentially desuccinylates peptides and the demyristoylating activity of Sir2Af2 is markedly faster than its deacetylating activity on a similar peptide. This finding underscores the principle that sirtuins are actually a family of deacylases, and suggests that future studies on other sirtuins will likely uncover alternate specificities as well.

Relative to its deacetylation activity, the archaeal sirtuin Sir2Af2 is more active against acyl chains of increasing length. This activity was suggested by previous structural studies revealing the presence of a hydrophobic tunnel adjacent to the active site that was occupied by a PEG molecule in a structure of Sir2Af2 bound to NAD$^+$.[38] However, in contrast with the desuccinylating enzymes Sir2Af1, SIRT5, and CobB, which contain a conserved R/Y
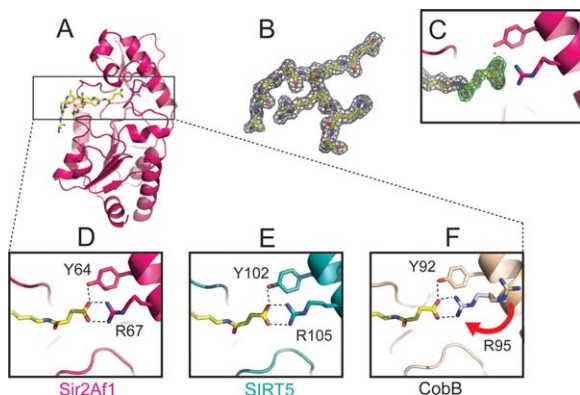
Figure 4. (a) Structure of Sir2Af1 bound to a succinylated peptide. (b) $2F_o$-F_c map of the succinylated peptide contoured at 1σ (gray). (c) Simulated annealing omit map of the succinyl group shows density for the modified lysine. $2F_o$-F_c map is colored gray and contoured at 1σ. F_o-F_c map is colored green and contoured at 3σ. (d) The hydrogen-bonding network in the active site of Sir2Af1 (pink) bound to a succinylated peptide (yellow) resembles (e) that for human SIRT5 (3RIY–teal) and (f) *E. coli* CobB (1S5P–wheat). For CobB, the position of the succinylated peptide comes from an alignment with the structure of Sir2Af1. Changing the rotamer for R95 in CobB (light blue) recapitulates the hydrogen-bonding network seen in the other two structures.

motif that confers specificity for a negatively charged acyl group, the ability of Sir2Af2, PfSir2a, and SIRT6 to accommodate long acyl chains is not the result of conserved sequence elements. When the amino acid sequences of these three enzymes are aligned along with other sirtuins with different specificities (Fig. 6), no pattern of sequence conservation emerges that distinguishes the demyristoylating enzymes. Of all the amino acid residues within 5 Å of the myristoyl acyl chain in the Sir2Af2 structure, the only residues that are conserved among the demyristoylating enzymes are also generally conserved among sirtuins (Fig. 6). Therefore, structural and biochemical studies remain the only way at present to identify sirtuins specific for removing long acyl chains.

Structural plasticity in the Sir2Af2 active site may facilitate its ability to accommodate and remove a broad array of acyl chains from lysine. In the structure of Sir2Af2 bound to an acetylated peptide,[38] the hydrophobic tunnel is too short to accommodate a myristoyl lysine [Fig. 5(e)], despite the fact that it efficiently catalyzes demyristoylation *in vitro* [Fig. 3(a)]. It is important to point out that shorter acyl chains such as butyryl or octanoyl lysine could likely still bind to Sir2Af2 in this conformation. However, its structure bound to a myristoylated peptide reveals a conformational change, which generates a long channel that extends through the entire enzyme and is open to solvent. In this new conformation, Sir2fAf2 may be able to accommodate an

aliphatic chain of greater length, raising the possibility that it could remove even longer acyl chains such as palmitic acid [Fig. 5(f)]. However, other structurally characterized sirtuins with open hydrophobic tunnels, like human SIRT6[31] and human SIRT2,[48] are still weak depalmitoylating enzymes,[33,48] suggesting that this modification may not be targeted by sirtuins in general.

Interestingly, crystal structures of SIRT6 and PfSir2a, which also remove long acyl chains from lysine, do not exhibit the same degree of structural flexibility as Sir2Af2 in this region. A comparison of the structures of SIRT6 alone (PDB ID 3K35), in complex with ADP-ribose (PDB ID 3PKI), or bound to a myristoylated peptide (PDB ID 3ZG6)[31] does not show any structural differences in the vicinity of the acyl modification. Likewise, crystal structures of PfSir2a have been determined bound to AMP (PDB ID 3JWP), to a myristoylated peptide (PDB ID 3U3D),[32] and to both a myristoylated peptide and NAD$^+$ (PDB ID 3U31),[32] all of which adopt similar conformations near the myristoyl chain.
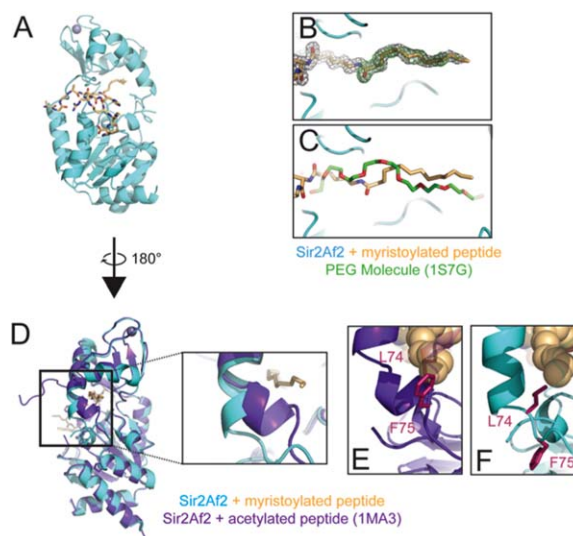

Figure 5. Structure of Sir2Af2 bound to a myristoylated peptide. (a) Overall structure with Sir2Af2 shown in cyan and myristoylated H4 peptide shown in yellow. (b) Simulated annealing omit map of the myristoyl group (yellow). $2F_o$-F_c map (gray) is contoured at 1σ and F_o-F_c map (green) is contoured at 2σ. (c) The myristoyl group (yellow) aligns with the PEG molecule in a previous structure of Sir2Af2 (green). (d) Overlay of the Sir2Af2 (cyan) bound to myristoylated peptide (yellow) with Sir2Af2 bound to an acetylated peptide (1MA3; purple). Inset shows structural rearrangement required to accommodate the myristoyl group. (e) The hydrophobic tunnel from the structure of Sir2Af2 (purple) bound to an acetylated peptide (1MA3) is occluded by L74 and F75 (magenta). Superimposed myristoyl group (yellow spheres) clashes with L74 and F75. (f) Conformational rearrangement when Sir2Af2 (cyan) is bound to a myristoylated peptide (yellow spheres) opens up the hydrophobic tunnel by moving the positions of L74 and F75 (magenta).
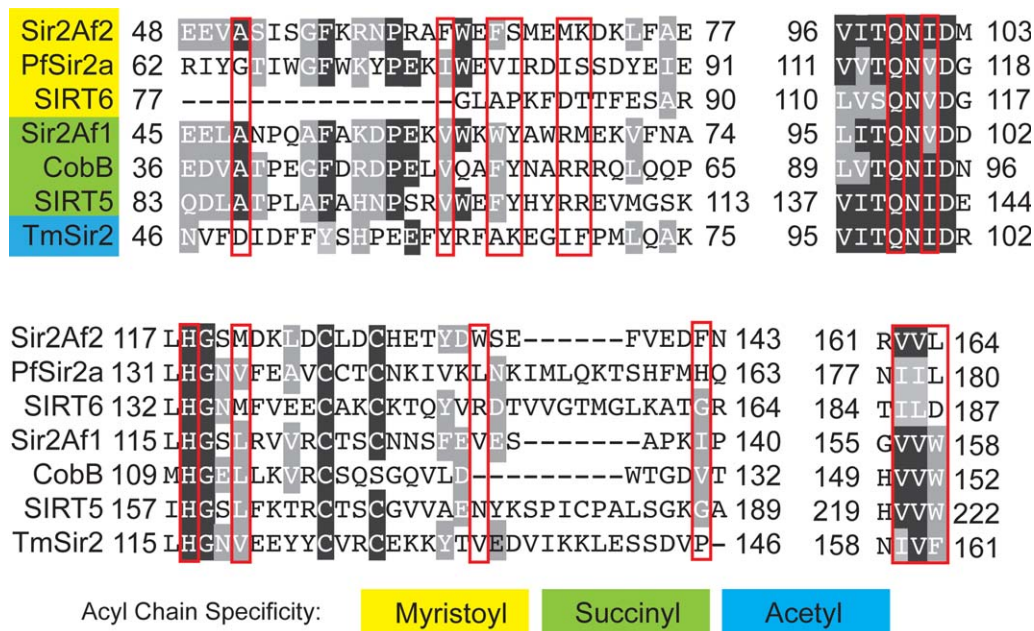
Figure 6. Sequence alignment among sirtuins with different acyl specificities performed using ClustalW. Residues within 5 Å of the myristoyl acyl chain are boxed in red.

The fact that Sir2Af2 must undergo a structural rearrangement to accommodate myristoyl lysine has important implications for studying the acyl specificity of other sirtuins, as it suggests that modeling substrates into preexisting structures will not be sufficient to predict the types of acyl chains targeted by a particular enzyme. Without directly testing the acyl specificity of Sir2Af2, its ability to remove very long chain acyl modifications would have been overlooked. These observations make clear that simply using docking programs may not capture the acyl chain preferences of many sirtuins with unknown specificities.

For other sirtuins like Sir2Af1, *E. coli* CobB, and human SIRT5, the presence of conserved sequence elements is sufficient to predict their specificity for negatively charged acyl chains. Here we make the surprising observation that Sir2Af1 and *E. coli* CobB, which are both desuccinylating enzymes, display incrementally slower kinetics with increasing acyl chain length, whereas the addition of a terminal carboxyl group to the acyl modification results in markedly higher deacylation rates. A similar pattern has been observed with human SIRT5, which has no detectable debutyrylating activity but robustly catalyzes desuccinylation.[33] This is counterintuitive, as one would expect that favorable hydrophobic interactions between the acyl chain and enzyme might give rise to the opposite effect. For example, butyryl lysine and succinyl lysine contain the same number of backbone carbons and differ only by the presence of a terminal carboxylate for succinyl lysine. However, Sir2Af1 deacylation activity is 12-fold faster on succinylated versus butyrylated substrates, but only

five-fold faster on acetylated versus butyrylated substrates (Supporting Information Table I). Since full kinetic and thermodynamic studies were not done, it remains to be seen whether these differences are also reflected in catalytic efficiency and how binding affinity for different acyl chains correlates with activity for these sirtuins.

TmSir2 was the only sirtuin of the four studied here that exhibited preferential deacetylase activity. Consistent with our findings, a previous study that characterized the kinetics and thermodynamics of TmSir2 against acetylated and propionylated substrates showed tighter binding but slower overall kinetics with the longer acyl chain.[47] Moreover, the active site of TmSir2 does not appear to be able to rearrange and accommodate longer acyl chains, demonstrated by a crystal structure of TmSir2 bound to a propionylated peptide.[47] Thus, while the ability to remove diverse acyl modification seems increasingly to be a characteristic of many sirtuins, some enzymes in this family appear to be bona fide deacetylases that are unlikely to remove larger acyl groups.

Promiscuity with regard to acyl chain specificity is emerging as a common feature of sirtuin enzymes, many of which are able to remove a number of chemically related acyl groups from lysine.[33,49] This has been explicitly shown for human SIRT1–6, which are each able to remove several types of acyl chains *in vitro*.[33] For example, human SIRT1 is able to efficiently remove acyl chains ranging in length from acetyl (two carbons) to myristoyl groups (14 carbons), although it is only weakly active against palmitoyl lysine (16 carbons) and ignores acyl chains

containing carboxylates or sulfhydryls.[33] Human SIRT5, which is very active against succinyl lysine, also removes a number of long acyl chains from lysine that vary in length from octanoylation (eight carbons) to dodecanoylation (12 carbons).[33] These data support the idea that promiscuity is a common feature of many sirtuin enzymes, and that this property has been conserved throughout evolution. Intriguingly, the deacetylating activity of human SIRT6, which preferentially removes acyl chains ranging in length from 6 to 14 carbons,[33] is strongly stimulated by free fatty acids.[33] This suggests that SIRT6-catalyzed deacetylation may be coupled to the concentration of various intracellular metabolites. It is likely that free fatty acids bind within the hydrophobic tunnel occupied by myristoyl lysine in the structure of SIRT6,[31] since myristic acid competitively inhibits SIRT6-catalyzed demyristoylation of histone peptides while stimulating SIRT6-catalyzed deacetylation of the same substrate.[33] Although not explicitly tested here, the archaeal sirtuin Sir2Af2 may also be regulated in this way, as it also contains a hydrophobic tunnel with the potential to bind free fatty acids.

While the biological functions for the archaeal sirtuins are not well characterized, it is clear that these enzymes are not simply deacetylases. There are likely other sirtuins whose true specificities remain to be discovered. Although the conserved Arg/Tyr sequence element can be used to predict specificity for negatively charged acyl chains,[16] biochemical, and structural studies remain the primary tool for predicting whether a sirtuin will accept long acyl chains in its active site. We expect that the identification of sirtuin enzymes with alternate specificities will keep pace with the discovery of new acyl modifications *in vivo*, as lysine acylation emerges as a common element of the signaling landscape in all three domains of life.[50]

Materials and Methods

Protein expression and purification

TmSir2 was expressed and purified as previously described.[51] Sir2Af2 was expressed and purified as previously described,[51] except that the Cibracron Blue column was run before the anion exchange (HiTrap Q, GE LifeSciences) column. Protein that bound to the Cibacron Blue column was concentrated and loaded on a Superdex 75 26/60 column. After gel filtration, fractions containing Sir2Af2 were dialyzed into 20 mM HEPES, pH 7.4, and 1 mM tris(2-carboxyethyl)phosphine (TCEP), concentrated to 20 mg/mL, and flash-frozen in liquid nitrogen. Sir2Af1 was purified as previously described[38] with the following modifications: after heating the cell lysate and passing the soluble portion over a HiTrap Q column (HiTrap Q HP 5 mLs, GE LifeSciences), the flow-through was bound to a 5 mL HiTrap SP column (GE LifeSciences) equilibrated in 20 mM MES, pH 6.0, 25 mM NaCl, and 1 mM dithiothreitol (DTT), and eluted with a linear gradient of 0.025 to 1M NaCl. Fractions containing Sir2Af1 were concentrated and loaded on a Superdex 75 26/60 (GE LifeSciences) in 20 mM HEPES, pH 8.0, 150 mM NaCl, 1 mM DTT, and 25 μM ZnCl$_2$. Sir2Af1 was concentrated to 20 mg/mL in the same buffer and flash-frozen in liquid nitrogen.

E. coli CobB aa1–279 was amplified by colony polymerase chain reaction (PCR) from XL1-Blue cells (Stratagene) and cloned as a thioredoxin-fusion into a pET32a vector (EMD Millipore, Merck KGaA, Darmstadt, Germany) with an N-terminal Tobacco Etch Virus (TEV) protease cleavage site and a four amino acid unstructured linker before the start codon (ENLYFQGASAS). Plasmid containing CobB was expressed in Rosetta-2(DE3)pLysS cells (EMD Millipore). Starter cultures were grown overnight in MDG media,[52] diluted into M9ZB[52] media for protein expression, and grown at 37°C to an OD$_{600nm}$ of 2.0. The cells were transferred to an ice bath for 45 min, induced by addition of 0.5 mM IPTG, and grown overnight at 15°C. Cells were lysed in 20 mM HEPES, pH 7.6, 500 mM NaCl, 5 mM β-mercaptoethanol (BME), and 20 mM Imidazole, and passed over a 5 mL HisTrap column (GE LifeSciences). CobB was eluted with a 20 to 400 mM imidazole gradient and dialyzed overnight at 4°C into 100 mM NaCl, 20 mM HEPES, pH 7.6, and 5 mM BME in the presence of 1 mg TEV protease per 20 mg recombinant protein. Cleaved protein was passed over a HisTrap column and the flow-through was further purified using a 5 mL Q HP column (GE LifeSciences) in 20 mM HEPES, pH 7.6, 50 mM NaCl, and 200 μM TCEP with a linear gradient of 0.2 to 1M NaCl. Fractions containing CobB were dialyzed into 20 mM HEPES, pH 7.6, 100 mM NaCl, and 200 μM TCEP, concentrated to 5 mg/mL, and flash-frozen in liquid nitrogen.

All peptides used in this study had the following sequence: KGLGKGGA-K*-RHRKW, corresponding to amino acids 8–20 of histone H4; K* indicates the position of the acylated lysine. The following acyl modifications were incorporated at the sixteenth position (K*): acetyl lysine, propionyl lysine, butyryl lysine, succinyl lysine, and myristoyl lysine. Peptides for biochemical assays were purchased at >70% purity from JPT Peptide Technologies GmBH (Berlin, Germany) and used without further purification. Peptides for crystallization were synthesized as previously described[32] in the Johns Hopkins University School of Medicine Synthesis and Sequencing Facility (Baltimore, MD), where they were HPLC purified to >90% purity. Peptide concentrations were determined with a spectrophotometer using a molar extinction coefficient of $\varepsilon_{280nm} = 5690$ M^{-1} cm^{-1}.

Deacylating Specificities of the Archaeal Sirtuins

Enzymatic activity assays

Enzyme-coupled assays monitoring NAD^+-consumption were performed as previously described with the following modifications[38]: Assays were run in buffer containing 100 mM HEPES, pH 8.0, 50 mM NaCl, 0.5 mM DTT, and 1 mM NAD^+ (Sigma N7004-1G) that had been neutralized with NaOH. Peptide stock solutions were made at 1 mM and used at a final concentration of 250 μM in the assays. Reactions were initiated with the addition of enzyme, which was used at a final concentration of 2 μM for TmSir2, CobB, and Sir2Af2, and at a concentration of 15 μM for Sir2Af1. Reactions containing the thermophilic sirtuins TmSir2, Sir2Af2, and Sir2Af1 were maintained at 50°C, and reactions containing CobB were maintained at 37°C; all reactions were run in a thermal cycler with heated lid to prevent sample evaporation. Glucose-6-phosphate (Sigma G7879-1G) and glucose-6-phosphate-dehydrogenase (Sigma G8529-2KU) were purchased from Sigma. For each rate measurement, six time points were collected initially to determine the range in which NAD^+-consumption was linear with time and steady-state conditions were met. Three to five time points within the linear time frame were then collected for each reaction. The remaining NAD+ was converted to NADH by addition of glucose-6-phosphate and G6PD as described[38] and the NADH concentration was determined by measuring the absorbance at 340 nm. To calculate v/[E], the concentration of NADH versus time was plotted, the data were fit to a line, and the slope of that line was normalized to enzyme concentration.

Reactions whose products were analyzed by high performance liquid chromatography (HPLC) were run in the same assay buffer as the enzyme-coupled assay. For Sir2Af2, 2 μM enzyme and 250 μM H4K16-myristoyl peptide were mixed in the presence and absence of 2 mM NAD^+ in a total reaction volume of 50 μL. Reactions were incubated for 20 min at 50°C, quenched with an equal volume of 10% TFA, placed on ice for 30 min, and spun twice for 10 min at room temperature at 18,000g to precipitate the enzyme. The reaction products were separated on a Kinetex XB-C18 column (100Å, 75 × 4.60 mm^2, 2.6 μm, Phenomenex) heated to 30°C using a 40–100% acetonitrile gradient in 0.1% triflouroacetic acid (TFA) developed at 0.5 mL/min over 20 min. Absorbance was monitored at 280 nm. For Sir2Af1, 15 μM enzyme and 250 μM H4K16-succinyl peptide were mixed in the presence and absence of 2 mM NAD^+ in a total reaction volume of 50 μL. Reactions were incubated for 60 min at 50°C, quenched with an equal volume of 0.5N HCl in methanol, incubated for >3 h at −20°C to precipitate the enzyme, and spun twice for 10 min each at 18,000g. The reaction products were separated on the same column as above using a 65–75% gradient,

where Buffer A contained 0.1% TFA and Buffer B contained 0.1% TFA and 95% methanol developed at 0.5 mL/min. Absorbance was monitored at 280 nm.

Crystallization, data collection, and refinement

For the crystal structure of Sir2Af1 bound to a succinylated peptide, equal volumes Sir2Af1 at 20 mg/mL and peptide (H4K16-succinyl) at 3 mM in 20 mM HEPES, pH 7.4 were mixed and incubated for >30 min on ice. The resulting mixture contained 10 mg/mL Sir2Af1 and 1.5 mM peptide. Crystals were grown by vapor diffusion at 20°C by mixing 1 μL of protein solution with 1 μL of well solution containing 0.1M Tris, pH 8.5, 200 mM $MgCl_2$, and 20% (w/v) PEG 8,000. Crystals grew in 3–5 days, were cryo-protected with the addition of glycerol to 30% (v/v), and flash frozen in a liquid nitrogen stream. Diffraction data were collected in-house using a Rigaku FR-E X-ray generator using X-rays with a wavelength of 1.54 Å and recorded with a Saturn 944+ detector. Crystals formed in primitive monoclinic space group P2$_1$ with unit cell dimensions $a = 44.61$ Å, $b = 51.36$ Å, $c = 57.69$ Å, and $\beta = 101.9°$.

For the crystal structure of Sir2Af2 bound to a myristoylated peptide, a mixture containing 10 mg/mL Sir2Af2, 1.5 mM H4K16-myrisotyl peptide, 10% (v/v) polystyrene nanospheres (Nanosphere Size Standards, Cat. No.: 3020A, ThermoScientific), 10 mM HEPES, pH 7.4, and 1 mM TCEP was incubated on ice for >30 min. The mixture precipitated upon addition of the nanospheres, but was still used to set trays. Crystals were grown by vapor diffusion at 20°C by mixing 1 μL protein solution with 1 μL well solution. The well solution contained 0.1M Na acetate, pH 4.8, 14–18% (v/v) 2-propanol, and 14–15% (w/v) PEG 6,000. Crystals grew to their final dimensions in 5–8 days and were cryo-protected with the addition of glycerol to 20% (v/v). Diffraction data on frozen crystals were collected at the GM/CA-CAT beamline 23-ID-D at the Advanced Photon Source using a wavelength of 1.033 Å. The complex crystallized in primitive monoclinic space group P2$_1$ with unit cell dimensions $a = 38.48$ Å, $b = 77.25$ Å, $c = 45.90$ Å, and $\beta = 110.7°$.

Both data sets were indexed and scaled with HKL2000[53] and structures were determined by molecular replacement with MOLREP from the CCP4 suite.[54–56] For the structure of Sir2Af1 bound to a succinylated peptide, the coordinates of Sir2Af1 (PDB ID 1ICI)[39] were used as a search model. For the structure of Sir2Af2 bound to a myristoylated peptide, the coordinates of Sir2Af2 (PDB ID 1MA3)[38] were used as a search model. Subsequent rounds of model-building and reciprocal space refinement were done with the graphics program COOT[57] and REFMAC5 from the CCP4 suite.[56,58] Crystallographic statistics are summarized in Table I. Simulated annealing omit maps were created by deleting the atoms corresponding to

the succinyl or myristoyl groups from the refined structures followed by three rounds of refinement with Phenix that included two cycles of simulated annealing.[59]

Coordinates have been deposited in the PDB with the accession codes 4TWI for Sir2Af1 bound to a succinylated peptide and 4TWJ for Sir2Af2 bound to a myristoylated peptide.

References

1. Choudhary C, Kumar C, Gnad F, Nielsen ML, Rehman M, Walther TC, Olsen JV, Mann M (2009) Lysine acetylation targets protein complexes and co-regulates major cellular functions. Science 325:834–840.

2. Lundby A, Lage K, Weinert BT, Bekker-Jensen DB, Secher A, Skovgaard T, Kelstrup CD, Dmytriyev A, Choudhary C, Lundby C, Olsen JV (2012) Proteomic analysis of lysine acetylation sites in rat tissues reveals organ specificity and subcellular patterns. Cell Rep 2: 419–431.

3. Zhang J, Sprung R, Pei J, Tan X, Kim S, Zhu H, Liu C-F, Grishin NV, Zhao Y (2009) Lysine acetylation is a highly abundant and evolutionarily conserved modification in *Escherichia coli*. Mol Cell Proteomics 8:215–225.

4. Jensen ON (2006) Interpreting the protein language using proteomics. Nat Rev Mol Cell Biol 7:391–403.

5. Olsen JV, Mann M (2013) Status of large-scale analysis of post-translational modifications by mass spectrometry. Mol Cell Proteomics 12:3444–3452.

6. Chen Y, Sprung R, Tang Y, Ball H, Sangras B, Kim SC, Falck JR, Peng J, Gu W, Zhao Y (2007) Lysine propionylation and butyrylation are novel post-translational modifications in histones. Mol Cell Proteomics 6:812–819.

7. Tan M, Luo H, Lee S, Jin F, Yang Jeong S, Montellier E, Buchou T, Cheng Z, Rousseaux S, Rajagopal N, Lu Z, Ye Z, Zhu Q, Wysocka J, Ye Y, Khochbin S, Ren B, Zhao Y (2011) Identification of 67 histone marks and histone lysine crotonylation as a new type of histone modification. Cell 146:1016–1028.

8. Xie Z, Dai J, Dai L, Tan M, Cheng Z, Wu Y, Boeke JD, Zhao Y (2012) Lysine succinylation and lysine malonylation in histones. Mol Cell Proteomics 11:100–107.

9. Peng C, Lu Z, Xie Z, Cheng Z, Chen Y, Tan M, Luo H, Zhang Y, He W, Yang K, Zwaans BMM, Tishkoff D, Ho L, Lombard D, He T-C, Dai J, Verdin E, Ye Y, Zhao Y (2011) The first identification of lysine malonylation substrates and its regulatory enzyme. Mol Cell Proteomics 10:M111.012658.

10. Zhang Z, Tan M, Xie Z, Dai L, Chen Y, Zhao T (2011) Identification of lysine succinylation as a new post-translational modification. Nat Chem Biol 7:58–63.

11. Tan M, Peng C, Anderson Kristin A, Chhoy P, Xie Z, Dai L, Park J, Chen Y, Huang H, Zhang Y, Ro J, Wagner Gregory R, Green Michelle F, Madsen Andreas S, Schmiesing J, Peterson Brett S, Xu G, Ilkayeva Olga R, Muehlbauer Michael J, Braulke T, Mühlhausen C, Backos Donald S, Olsen Christian A, McGuire Peter J, Pletcher Scott D, Lombard David B, Hirschey Matthew D, Zhao Y (2014) Lysine glutarylation is a protein post-translational modification regulated by SIRT5. Cell Metab 19:605–617.

12. Weinert Brian T, Schölz C, Wagner Sebastian A, Iesmantavicius V, Su D, Daniel Jeremy A, Choudhary C (2013) Lysine succinylation is a frequently occurring modification in prokaryotes and eukaryotes and extensively overlaps with acetylation. Cell Rep 4:842–851.

13. Colak G, Xie Z, Zhu AY, Dai L, Lu Z, Zhang Y, Wan X, Chen Y, Cha YH, Lin H, Zhao Y, Tan M (2013) Identification of lysine succinylation substrates and the succinylation regulatory enzyme CobB in *Escherichia coli*. Mol Cell Proteomics 12:3509–3520.

14. Garrity J, Gardner JG, Hawse W, Wolberger C, Escalante-Semerena JC (2007) N-Lysine propionylation controls the activity of propionyl-CoA synthetase. J Biol Chem 282:30239–30245.

15. Rardin MJ, He W, Nishida Y, Newman JC, Carrico C, Danielson SR, Guo A, Gut P, Sahu AK, Li B, Uppala R, Fitch M, Riiff T, Zhu L, Zhou J, Mulhern D, Stevens RD, Ilkayeva OR, Newgard CB, Jacobson MP, Hellerstein M, Goetzman ES, Gibson BW, Verdin E (2013) SIRT5 regulates the mitochondrial lysine succinylome and metabolic networks. Cell Metab 18:920–933.

16. Du J, Zhou Y, Su X, Yu JJ, Khan S, Jiang H, Kim J, Woo J, Kim JH, Choi BH, He B, Chen W, Zhang S, Cerione RA, Auwerx J, Hao Q, Lin H (2011) Sirt5 is a NAD-dependent protein lysine demalonylase and desuccinylase. Science 334:806–809.

17. Smith JS, Brachmann CB, Celic I, Kenna MA, Muhammad S, Starai VJ, Avalos JL, Escalante-Semerena JC, Grubmeyer C, Wolberger C, Boeke JD (2000) A phylogenetically conserved NAD+-dependent protein deacetylase activity in the Sir2 protein family. Proc Natl Acad Sci U S A 97:6658–6663.

18. Frye RA (2000) Phylogenetic classification of prokaryotic and eukaryotic Sir2-like proteins. Biochem Biophys Res Commun 273:793–798.

19. Greiss S, Gartner A (2009) Sirtuin/Sir2 phylogeny, evolutionary considerations and structural conservation. Mol Cells 28:407–415.

20. Braunstein M, Rose AB, Holmes SG, Allis CD, Broach JR (1993) Transcriptional silencing in yeast is associated with reduced nucleosome acetylation. Genes Dev 7:592–604.

21. Li R, Gu J, Chen Y-Y, Xiao C-L, Wang L-W, Zhang Z-P, Bi L-J, Wei H-P, Wang X-D, Deng J-Y, Zhang X-E (2010) CobB regulates Escherichia coli chemotaxis by deacetylating the response regulator CheY. Mol Microbiol 76:1162–1174.

22. Starai VJ, Celic I, Cole RN, Boeke JD, Escalante-Semerena JC (2002) Sir2-dependent activation of acetyl-CoA synthetase by deacetylation of active lysine. Science 298:2390–2392.

23. Zhang Q, Gu J, Gong P, Wang X, Tu S, Bi L, Yu Z, Zhang Z, Cui Z, Wei H, Tao S, Zhang X (2013) Reversibly acetylated lysine residues play important roles in the enzymatic activity of *Escherichia coli* N-hydroxyarylamine O-acetyltransferase. FEBS J 280: 1966–1979.

24. Lima BP, Antelmann H, Gronau K, Chi BK, Becher D, Brinsmade SR, Wolfe AJ (2011) Involvement of protein acetylation in glucose-induced transcription of a stress-responsive promoter. Mol Microbiol 81:1190–1204.

25. Hu LI, Chi BK, Kuhn ML, Filippova EV, Walker-Peddakotla AJ, Bäsell K, Becher D, Anderson WF, Antelmann H, Wolfe AJ (2013) Acetylation of the response regulator RcsB controls transcription from a small RNA promoter. J Bacteriol 195:4174–4186.

26. Thao S, Chen C-S, Zhu H, Escalante-Semerena JC (2010) Lysine acetylation of a bacterial transcription factor inhibits its DNA-binding activity. PLoS ONE 5: e15123.

27. Michan S, Sinclair D (2007) Sirtuins in mammals: insights into their biological function. Biochem J 404: 1–13.

28. Vassilopoulos A, Fritz K, Petersen D, Gius D (2011) The human sirtuin family: evolutionary divergences and functions. Hum Genomics 5:485–496.

29. Sauve AA, Wolberger C, Schramm VL, Boeke JD (2006) The biochemistry of sirtuins. Annu Rev Biochem 75:435–465.

30. Houtkooper RH, Pirinen E, Auwerx J (2012) Sirtuins as regulators of metabolism and healthspan. Nat Rev Mol Cell Biol 13:225–238.

31. Jiang H, Khan S, Wang Y, Charron G, He B, Sebastian C, Du J, Kim R, Ge E, Mostoslavsky R, Hang HC, Hao Q, Lin H (2013) SIRT6 regulates TNF-alpha secretion through hydrolysis of long-chain fatty acyl lysine. Nature 496:110–113.

32. Zhu AY, Zhou Y, Khan S, Deitsch KW, Hao Q, Lin H (2011) Plasmodium falciparum Sir2A preferentially hydrolyzes medium and long chain fatty acyl lysine. ACS Chem Biol 7:155–159.

33. Feldman JL, Baeza J, Denu JM (2013) Activation of the protein deacetylase SIRT6 by long-chain fatty acids and widespread deacylation by mammalian sirtuins. J Biol Chem 288:31350–31356.

34. Park J, Chen Y, Tishkoff Daniel X, Peng C, Tan M, Dai L, Xie Z, Zhang Y, Zwaans Bernadette MM, Skinner Mary E, Lombard David B, Zhao Y (2013) SIRT5-mediated lysine desuccinylation impacts diverse metabolic pathways. Mol Cell 50:919–930.

35. Lin Z-F, Xu H-B, Wang J-Y, Lin Q, Ruan Z, Liu F-B, Jin W, Huang H-H, Chen X (2013) SIRT5 desuccinylates and activates SOD1 to eliminate ROS. Biochem Biophys Res Commun 441:191–195.

36. Michishita E, McCord RA, Berber E, Kioi M, Padilla-Nash H, Damian M, Cheung P, Kusumoto R, Kawahara TL, Barrett JC, Chang HY, Bohr VA, Ried T, Gozani O, Chua KF (2008) SIRT6 is a histone H3 lysine 9 deacetylase that modulates telomeric chromatin. Nature 452:492–496.

37. Dominy JE Jr, Lee Y, Jedrychowski MP, Chim H, Jurczak MJ, Camporez JP, Ruan HB, Feldman J, Pierce K, Mostoslavsky R, Denu JM, Clish CB, Yang X, Shulman GI, Gygi SP, Puigserver P (2012) The deacetylase Sirt6 activates the acetyltransferase GCN5 and suppresses hepatic gluconeogenesis. Mol Cell 48:900–913.

38. Avalos JL, Celic I, Muhammad S, Cosgrove MS, Boeke JD, Wolberger C (2002) Structure of a Sir2 enzyme bound to an acetylated p53 peptide. Mol Cell 10:523–535.

39. Min J, Landry J, Sternglanz R, Xu R-M (2001) Crystal structure of a SIR2 homolog–NAD complex. Cell 105:269–279.

40. Zhao K, Chai X, Marmorstein R (2004) Structure and substrate binding properties of cobB, a Sir2 homolog protein deacetylase from *Escherichia coli*. J Mol Biol 337:731–741.

41. Avalos JL, Bever KM, Wolberger C (2005) Mechanism of sirtuin inhibition by nicotinamide: Altering the NAD+ cosubstrate specificity of a Sir2 enzyme. Mol Cell 17:855–868.

42. Cosgrove MS, Bever K, Avalos JL, Muhammad S, Zhang X, Wolberger C (2006) The structural basis of sirtuin substrate affinity. Biochemistry 45:7511–7521.

43. Chang JH, Kim HC, Hwang KY, Lee JW, Jackson SP, Bell SD, Cho Y (2002) Structural basis for the NAD-dependent deacetylase mechanism of Sir2. J Biol Chem 277:34489–34498.

44. Avalos JL, Boeke JD, Wolberger C (2004) Structural basis for the mechanism and regulation of Sir2 enzymes. Mol Cell 13:639–648.

45. Fischer F, Gertz M, Suenkel B, Lakshminarasimhan M, Schutkowski M, Steegborn C (2012) Sirt5 deacylation activities show differential sensitivities to nicotinamide inhibition. PLoS One 7:e45098.

46. Hawse WF, Wolberger C (2009) Structure-based mechanism of ADP-ribosylation by sirtuins. J Biol Chem 284:33654–33661.

47. Bheda P, Wang JT, Escalante-Semerena JC, Wolberger C (2011) Structure of Sir2Tm bound to a propionylated peptide. Protein Sci 20:131–139.

48. Moniot S, Schutkowski M, Steegborn C (2013) Crystal structure analysis of human Sirt2 and its ADP-ribose complex. J Struct Biol 182:136–143.

49. Smith BC, Denu JM (2007) Acetyl-lysine analog peptides as mechanistic probes of protein deacetylases. J Biol Chem 282:37256–37265.

50. Choudhary C, Weinert BT, Nishida Y, Verdin E, Mann M (2014) The growing landscape of lysine acetylation links metabolism and cell signalling. Nat Rev Mol Cell Biol 15:536–550.

51. Smith JS, Avalos J, Celic I, Muhammad S, Wolberger C, Boeke JD (2002) SIR2 family of NAD+-dependent protein deacetylases. Methods Enzymol 353:282–300.

52. Studier FW (2005) Protein production by auto-induction in high-density shaking cultures. Protein Express Purif 41:207–234.

53. Otwinowski Z, Minor W, Processing of X-ray diffraction data collected in oscillation mode. In: Carter CW, Jr, Ed. (1997) Methods enzymol. New York: Academic Press, pp 307–326.

54. Vagin A, Teplyakov A (2010) Molecular replacement with MOLREP. Acta Cryst D66:22–25.

55. Vagin A, Teplyakov A (1997) MOLREP: An automated program for molecular replacement. J Appl Cryst 30:1022–1025.

56. Winn MD, Ballard CC, Cowtan KD, Dodson EJ, Emsley P, Evans PR, Keegan RM, Krissinel EB, Leslie AGW, McCoy A, McNicholas SJ, Murshudov GN, Pannu NS, Potterton EA, Powell HR, Read RJ, Vagin A, Wilson KS (2011) Overview of the CCP4 suite and current developments. Acta Cryst D67:235–242.

57. Emsley P, Cowtan K (2004) Coot: model-building tools for molecular graphics. Acta Cryst D60:2126–2132.

58. Murshudov GN, Vagin AA, Dodson EJ (1997) Refinement of macromolecular structures by the maximum-likelihood method. Acta Cryst D53:240–255.

59. Adams PD, Afonine PV, Bunkoczi G, Chen VB, Davis IW, Echols N, Headd JJ, Hung L-W, Kapral GJ, Grosse-Kunstleve RW, McCoy AJ, Moriarty NW, Oeffner R, Read RJ, Richardson DC, Richardson JS, Terwilliger TC, Zwart PH (2010) PHENIX: a comprehensive Python-based system for macromolecular structure solution. Acta Cryst D66:213–221.